Particle-bearing currents in uniform density and two-layer fluids

Bruce R. Sutherland,[1,2,*] Murray K. Gingras,[2] Calla Knudson,[2] Luke Steverango,[3] and Christopher Surma[4]

[1]*Department of Physics, University of Alberta, Edmonton, Alberta, Canada T6G 2E1*
[2]*Department of Earth and Atmospheric Sciences, University of Alberta, Edmonton, Alberta, Canada T6G 2E3*
[3]*Department of Mathematics and Statistics, McGill University, Montreal, Quebec, Canada H3A 0B9*
[4]*Department of Mechanical Engineering, University of Alberta, Edmonton, Alberta, Canada T6G 1H9*

(Received 18 December 2017; published 23 February 2018)

Lock-release gravity current experiments are performed to examine the evolution of a particle bearing flow that propagates either in a uniform-density fluid or in a two-layer fluid. In all cases, the current is composed of fresh water plus micrometer-scale particles, the ambient fluid is saline, and the current advances initially either over the surface as a hypopycnal current or at the interface of the two-layer fluid as a mesopycnal current. In most cases the tank is tilted so that the ambient fluid becomes deeper with distance from the lock. For hypopycnal currents advancing in a uniform density fluid, the current typically slows as particles rain out of the current. While the loss of particles alone from the current should increase the current's buoyancy and speed, in practice the current's speed decreases because the particles carry with them interstitial fluid from the current. Meanwhile, rather than settling on the sloping bottom of the tank, the particles form a hyperpycnal (turbidity) current that advances until enough particles rain out that the relatively less dense interstitial fluid returns to the surface, carrying some particles back upward. When a hypopycnal current runs over the surface of a two-layer fluid, the particles that rain out temporarily halt their descent as they reach the interface, eventually passing through it and again forming a hyperpycnal current. Dramatically, a mesopycnal current in a two-layer fluid first advances along the interface and then reverses direction as particles rain out below and fresh interstitial fluid rises above.

DOI: 10.1103/PhysRevFluids.3.023801

I. INTRODUCTION

Most rivers that run into the ocean carry with them suspended clay and silt, as well as possible chemical and/or particulate by-products of agriculture and industry [1]. Although the particles are more dense than saline ocean water, the suspended sediment concentration in rivers is typically so small that the outflow, known as a river plume, is buoyant and propagates over the surface of the ocean water as a hypopycnal current [2]. However, the particles do eventually rain out of the current. Observations of the sea surface near a river outflow show the appearance of well-defined fronts with high particle concentration on the landward side and weak to no particle concentration on the seaward side [3–5]. Subsurface observations are difficult to obtain and consequently little is known about the evolution of these particle-bearing flows after the particles descend from the surface, although inferences have been made based on observed sedimentary depositions (for a recent example, see Ref. [6]). Qualitative insights into some aspects of the evolution of hypopycnal currents have been gained by laboratory experiments of particle bearing flows initially passing over

*bruce.sutherland@ualberta.ca; https://www.ualberta.ca/~bsuther

a uniform-density ambient fluid [7–9]. In particular, Parsons *et al.* [8] and Snow and Sutherland [9] showed that particles settling from a hypopycnal current do not come to rest at the bottom directly beneath their settling location. Instead, they can form a hyperpycnal current (also called a turbidity current or hyperpycnite) that continues to propagate horizontally or downslope until particles rain out of this flow. Even here it is possible for the relatively light interstitial fluid of the hyperpycnal current to rise again after sufficient particle settling has occurred and, in so doing, carry some particles back upward into the fluid column. Here our primary intent is to provide quantitative insight into the evolution of hypopycnal currents and consequent hyperpycnal currents. As a step toward the more realistic circumstance of river plumes flowing into stratified oceans and lakes, we further qualitatively explore the more complicated dynamics of particle-bearing currents released into a two-layer stratified ambient fluid.

Our approach is to perform lock-release experiments in which a mixture of particles and fresh water is impulsively released into a stationary saline fluid. There is a long history of research into particle-bearing and particle-driven currents formed through lock-release experiments. In some, the interstitial fluid in the lock was the same as that of the ambient fluid and so the particle-driven current advanced along the bottom until the particles rained out and the current stopped [10,11]. In others, the interstitial fluid was lighter than the ambient fluid, but the concentration of dense particles in the lock was sufficiently large that the net lock density was greater than that of the ambient fluid [12]. In these cases the current initially ran along the bottom until a sufficient mass of particles rained out that the current suddenly stopped and the interstitial fluid rose, carrying some particles with it. Such studies have been motivated to gain an understanding of the dynamics of pyroclastic flows emanating from volcanic eruptions. In experiments closer to the study presented here, the interstitial fluid was lighter than the ambient fluid and the particle concentration was sufficiently small that the net lock density was lighter than that of the ambient fluid [7]. In this case the current initially flowed along the surface as a hypopycnal current until particles rained out. One might expect the loss of particles to make the current less dense and so result in its horizontal acceleration. However, experiments show that the descending particles carry interstitial fluid down with them [7–9]. The so-depleted hypopycnal current eventually slows down due to its net loss of mass and buoyancy. The slowing is accentuated by a near-surface return flow that develops in response to the development of an underlying hyperpycnal current, formed by the descending particles as they approached the bottom of the tank [7].

From his experimental data, Maxworthy [7] attempted to quantify the advance in time of the current front position. While he found a partial collapse of data after scaling by the characteristic gravity current speed, he found that the stopping distance depended upon the ratio R of the reduced gravity of ambient to lock fluid over the reduced gravity of lock to interstitial fluid. Likewise, the sedimentation velocity compared to the Stokes settling velocity was found to depend upon R as well as the density contrast between the ambient and interstitial fluid. Because these experiments were performed using particles (carbonundum powder) with a fixed density of 3.2 g/cm^3 and mean diameter of 6.7 μm, he was unable to explore how the stopping distance was affected by the particle size.

Since the time of those experiments, it has become clear that particle settling from fluid of one density to another is a remarkably complex process. Besides the dynamics of double diffusion and convective settling [13–16], individual particles are influenced by interstitial fluid carried in a viscous sheath around each particle [17,18], this influence being more significant for particles of smaller size. The viscous sheath further influences the collective settling of particles in stratified fluids [19,20]. The dynamics are more complicated still if, like clay, the particles have a tendency to flocculate due to electrostatic interactions between the particles [21–23].

The main focus of our experiments is to further the quantitative analyses of Maxworthy [7] by examining the influence of particle size and concentration on the evolution of a hypopycnal current. After describing the experiment setup and analysis methods in Sec. II, in Sec. III we combine scaling analyses with semiempirical fits to data in order to predict the current speed and stopping distance of the hypopycnal current. We further develop semiempirical theories for the evolution of the

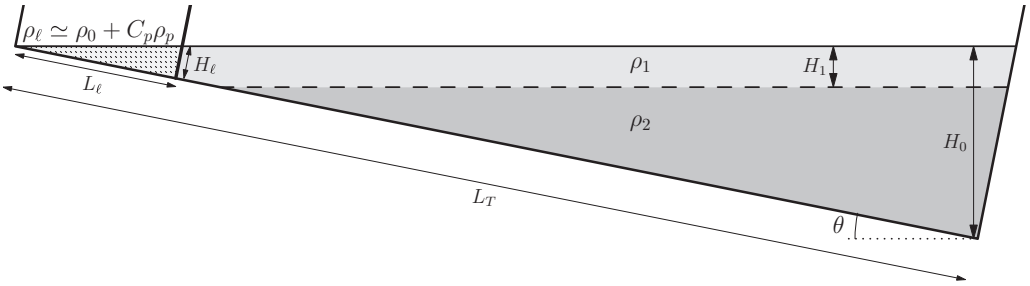

FIG. 1. Schematic of the setup in general for experiments performed in a rectangular tank tilted at an angle θ to the horizontal of particle-bearing fresh water currents released from a triangular lock of length L_ℓ and height H_ℓ into a uniform-density or two-layer ambient fluid. In the case of a two-layer ambient (pictured), an upper layer with depth H_1 of salty fluid having density ρ_1 overlies still saltier fluid having density ρ_2. In most experiments the ambient has uniform density such that $\rho_\ell < \rho_1$ (hypopycnal flow). In experiments with a two-layer ambient fluid either $\rho_\ell < \rho_1$ (hypopycnal flow) or $\rho_1 < \rho_\ell < \rho_2$ (mesopycnal flow).

hyperpycnal current that develops below the arrested hypopycnal current. In Sec. IV we demonstrate qualitatively the significant influence of interstitial fluid transport by settling particles upon the large-scale evolution of particle-bearing flows in a two-layer fluid. Our results are summarized in Sec. V.

II. EXPERIMENT SETUP AND ANALYSIS METHODS

A schematic of the experimental setup is shown in Fig. 1. A tank of length L_T was tilted an angle θ from the horizontal. A gate with edges covered with foam insulating tape was inserted a distance L_ℓ from the elevated corner of the tank. In experiments with a uniform density ambient fluid, salt water of density ρ_1 was filled to depth H_0 with respect to the bottom corner of the tank to the right of the gate and fresh water of density ρ_0 was poured into the lock on the left side of the gate. To prevent fluid from passing through the corners underneath the gate, plasticine was pressed into the corners of the tank at the location of the gate and the gate was pressed into the plasticine to form a tight seal. The initial surface heights of the ambient and lock fluids were the same. In experiments with $\theta = 0$ (the tank being untilted), the height H_0 was set arbitrarily. In tilted tank experiments with $\theta > 0$, the height was set so that the surface was level with the left corner of the tank (i.e., $H_0 = L_T \sin\theta$). In experiments with a two-layer ambient fluid, very salty fluid of density ρ_2 was filled to a depth below the bottom of the gate. Then moderately salty fluid of density ρ_1 was layered on top by passing it through a sponge float until the total ambient fluid depth was H with upper-layer depth H_1. The densities of the upper- and lower-layer ambient fluids were measured to five-digit accuracy using an Anton Paar DMA 4500 densitometer.

Shortly before an experiment began, a prescribed mass of particles with density ρ_p was added to the fresh water in the lock. In some experiments, five to ten drops of red or blue food coloring was additionally added to the lock fluid. The resulting density of the lock fluid was

$$\rho_\ell \simeq \rho_0 + \phi_p\rho_p, \tag{1}$$

in which ϕ_p is the concentration of particles by volume and the expression assumes that this concentration is small. In most experiments $\rho_\ell < \rho_1$, so the lock fluid after release formed a hypopycnal current. In experiments examining the evolution of mesopycnal currents, the lock-fluid density was intermediate between the upper- and lower-layer ambient fluid densities: $\rho_1 < \rho_\ell < \rho_2$.

To ensure the particles were well-distributed before release, the lock fluid was continuously stirred until just before the gate was extracted. Although the result of mixing the fluid up until extraction of the gate and the consequence of extracting the gate itself resulted in the generation of small-amplitude

surface waves, we found that their presence had negligible impact upon the current evolution by comparing similar experiments with small- and moderately-large-amplitude excited surface waves.

Overall, 55 uniform ambient fluid and 19 two-layer ambient fluid experiments were performed. Most experiments were performed in an acrylic tank of length $L_T = 122.2$ cm, height $H_T = 20.4$ cm, and width $W_T = 7.8$ cm. The tank was tilted so that its bottom formed an angle θ to the horizontal with θ ranging between 0 and 9.5°. In most experiments the tilt was set to be $\theta = 8°$. The gate was positioned at distances from the elevated left corner of the tank so that the lock height ranged between $H_\ell = 1.5$ and 12.0 cm, with most having $H_\ell = 3.0$ cm. In experiments with a uniform density ambient, the salt water density ranged from $\rho_1 = 1.01$ to 1.14 g/cm^3, with most experiments having $\rho_1 = 1.03$ g/cm^3. In all experiments with a two-layer fluid, the upper-layer density was $\rho_1 = 1.030$ g/cm^3 and the lower layer had a density ranging between $\rho_2 = 1.035$ and 1.060 g/cm^3. In these experiments the lock height was $H_\ell = 3$ cm in all cases but one that had $H_\ell = 12$ cm. The upper-layer height ranged from $H_1 = 1.0$ to 6.0 cm with most experiments having $H_1 = H_\ell = 3$ cm.

The particles themselves in most experiments consisted of glass ballotini with mean diameters ranging from $\bar{d}_p \simeq 11$ to 30 μm and having a density of $\rho_p = 2.4$ g/cm^3. Some experiments were performed using silicon carbide (SiC), which has a density of $\rho_p = 3.1$ g/cm^3 and a mean particle size of $\bar{d}_p = 7.8$ μm [16]. Like glass ballotini, particles of silicon carbide are monodispersed and noncohesive in fresh- or salt-water solutions. Experiments were also performed with three types of naturally occurring sediments (primarily clay, but also containing silt, diatoms, particulate iron, etc). These samples included clay gathered from the bottom of a Petitcodiac River channel ($\rho_p \simeq 2.52$ g/cm^3 and $\bar{d}_p \simeq 15$ μm), silty clay gathered from a cliff face adjacent to the Petitcodiac River ($\rho_p \simeq 2.50$ g/cm^3 and $\bar{d}_p \simeq 30$ μm), and Montmorillonite clay ($\rho_p \simeq 2.03$ g/cm^3 and $\bar{d}_p \simeq 20$ μm). These mean particle sizes were estimated from clay aggregates (flocs) imaged using a scanning electron microscope. Individually, particles of clay have the shape of plates with thickness much smaller than their lateral extent. The plates have an electrostatic charge that combines them into flocs. Particularly in the presence of salt water [22], the particles can flocculate to greater size and so enhance their settling rate. Such dynamics are complicated, and so here we focus most of our attention upon experiments performed using glass ballotini. In all experiments the mass of particles added to the lock was sufficiently small that the volume concentration ϕ_p was no greater than 2.5%. Thus settling in a uniform density fluid would not be affected by particle-particle interactions. However, we find that particles do interact as they settle from the current into the underlying denser ambient fluid [8,16].

A typical experiment of a hypopycnal current propagating into a uniform-density ambient fluid is shown in Fig. 2. Fifteen seconds after release [Fig. 2(b)], the hypopycnal current extended as a tongue of near-constant thickness between the nose and the far lee. Particle settling out of the current was apparent only after this time and occurred nearly uniformly over the horizontal extent of the current except near the current nose. By $t = 45$ s the settling particles accumulated along the bottom slope and the hypopycnal current at the surface slowed to a near halt. One might expect that the loss of particles from the current, which would make its density closer to that of fresh water, would result in acceleration of the more buoyant current. That in fact the current slowed down indicates that the descending particles carried a significant volume of fresh water down with them in the viscous boundary layers surrounding the particles, as has been observed earlier in experiments with a single large particle settling through a density interface [18].

By $t = 60$ s a bottom-propagating hyperpycnal current formed. This was composed of both particles and interstitial fluid that was a combination of the fresh water drawn down by the particles and the saline ambient which had mixed with this fluid. Consequently, as particles in the hyperpycnal current continued to settle to the tank bottom, the remaining interstitial fluid became lighter than its surroundings and, around $t = 180$ s, began to rise back to the surface, carrying some particles back up with it. Such dynamics have been observed in real and experimentally modeled pyroclastic flows [12,24]. The formation of a hyperpycnal current from a hypopycnal current was first noted by Parsons *et al.* [8]. This, and the consequent halting of the hyperpycnal current, was noted by Snow and Sutherland [9].

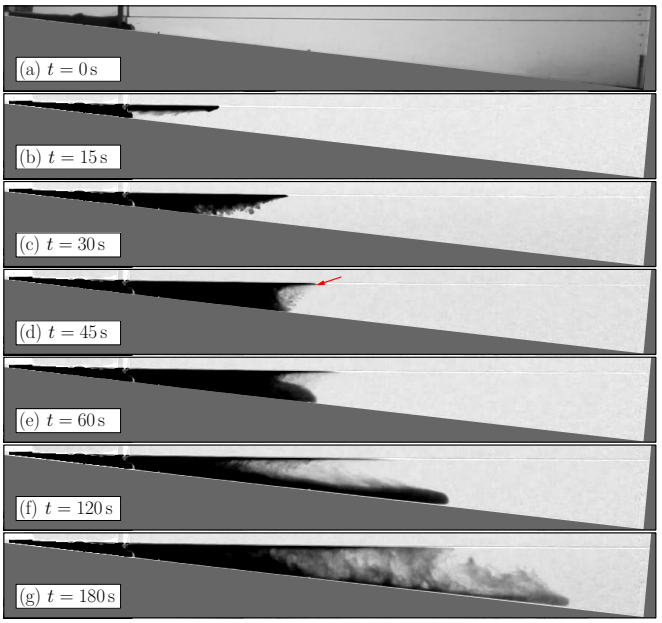

FIG. 2. Snapshots from an experiment of a hypopycnal current of fresh water with suspended glass ballotini advancing into a uniform density saline ambient at (a) $t = 0$ s, (b) $t = 15$ s, (c) $t = 30$ s, (d) $t = 45$ s, (e) $t = 60$ s, (f) $t = 120$ s, and (g) $t = 180$ s. The experiment parameters for the tank slope, lock height, and ambient density are $\theta = 6^\circ$, $H_\ell = 2.3$ cm, and $\rho_1 = 1.0310\,\mathrm{g/cm^3}$. The lock fluid has 2.2 g of $d_p = 11$ μm ballotini added to the fresh water in the lock, giving it a lock density of $\rho_\ell = 1.0051\,\mathrm{g/cm^3}$. The red arrow in (d) points at the stopping location measured from horizontal time series. The stopping time occurs at $t = 37$ s.

Part of the intent of this paper is to quantify these processes. To determine the speed and near-halting locations of the fronts, we constructed time series of the along-surface and along-bottom flows. For the experiment in Fig. 2, the corresponding time series are shown in Fig. 3.

The along-surface time series shown in Fig. 3(a) was constructed by stacking successive horizontal slices through snapshots of the experiment taken 1 mm below the surface. At early times this clearly shows a near-constant advance of the nose of the hypopycnal current until $t \simeq 50$ s, when the current rapidly slowed to a near halt at $t \simeq 60$ s. Although particles fell out of the hypopycnal current drawing some of the interstitial fluid with them, the current front nonetheless slowly advanced due to the buoyancy of the relatively low-density but shallow-depth head.

The along-slope time series shown in Fig. 3(b) illustrates that particles rained onto the slope arriving, in this case, at nearly the same time, around $t \simeq 40$ s. The formation of a hyperpycnal current front is evident around $t \simeq 50$ s. This propagated downslope at near-constant speed until it approached the far end of the tank, slowing to a halt at $x \simeq 90$ cm.

III. QUANTITATIVE RESULTS FOR CURRENTS IN UNIFORM DENSITY FLUID

From the time series images, like those shown in Fig. 3, we determined the initial speeds of the surface and hyperpycnal currents as well as their stopping distances for those experiments where the hyperpycnal current stopped before reaching the end wall of the tank. These quantitative analyses are performed only for experiments in which a hypopycnal current was released into a uniform-density ambient fluid.

The speed of the hypopycnal current is found from the slope of the best-fit line through measurements of the front position versus time [e.g., the white curve in Fig. 3(a)] taken up to one lock length from the gate. The measured speeds are compared in Fig. 4 with the prediction for

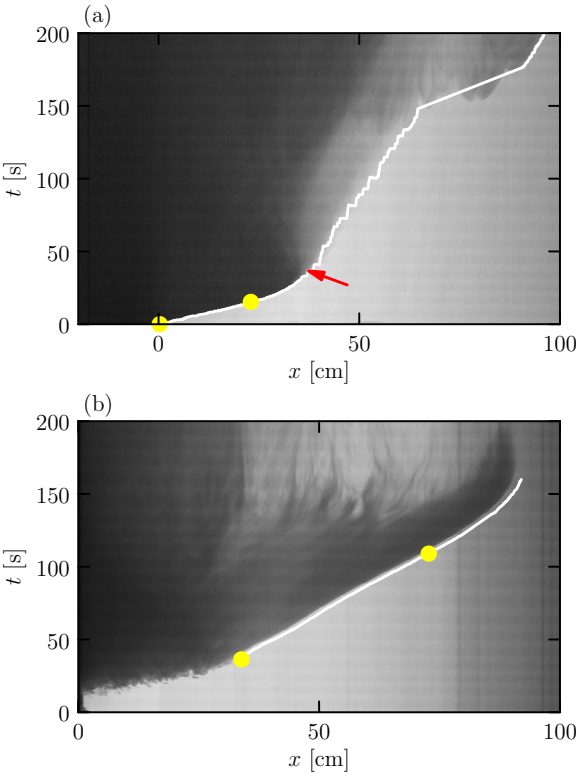

FIG. 3. (a) Along-surface and (b) along-slope time series taken from an experiment with snapshots shown in Fig. 2. The white lines in both images indicate the position of the front over time where the intensity decreases significantly due to a change in particle concentration with x. In (b) this is drawn only after formation of the hyperpycnal current. The closed circles in (a) and (b) indicate the start and end locations between which a best-fit line is found to the front position. The red arrow in (a) indicates where the front is taken to come to a near halt.

energy-conserving gravity currents released from a full-depth rectangular lock [25,26]. Explicitly, the speed is predicted to be

$$U_0 = \tfrac{1}{2}\sqrt{g' H_\ell}, \tag{2}$$

in which $g' = g(\rho_\ell - \rho_1)/\rho_\ell$ is the reduced gravity, the lock density ρ_ℓ is given by (1), and H_ℓ is the depth of the lock fluid at the gate.

The results include experiments performed with several different types and concentrations of particles. The observed speed generally agrees well with the theory for the speed of energy-conserving gravity currents in their slumping (steady) phase. Considering that the lock had a triangular instead of rectangular vertical cross section and that the lock-fluid was agitated to keep particles in suspension right up to the moment that the gate was extracted, this provides a good indication that the particles were indeed well mixed and remained in suspension within the current as it propagated more than one lock length from the gate.

To predict how far the current propagates from the gate before coming to a near halt, we take a box-model approach. We assume that entrainment into the current is negligible so that its vertical cross-sectional area $A_\ell \equiv H_\ell L_\ell/2 = h x_f$ is constant while its height h decreases and the distance x_f of the front from the left end of the tank increases. Also assuming that the current's propagation

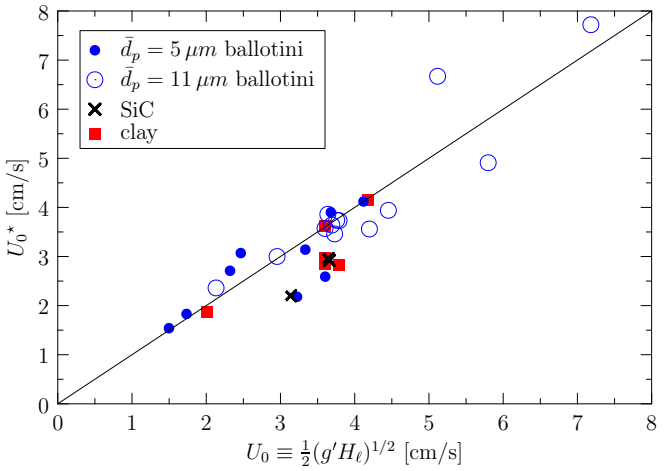

FIG. 4. Measured initial speed of hypopycnal current compared with theory for hypopycnal currents of fresh water mixed with particles consisting of 5-μm-diam (closed circles) and 11-μm-diam (open circles) glass spheres, particles of silicon carbide (crosses), and different clay samples. The diagonal black line is the one-to-one line where observations match theory.

speed is constant and given by (2), the change in current thickness with time is given by

$$\frac{dh}{dt} = -A_\ell U_0 / x_f^2. \tag{3}$$

The current is assumed to slow when particles are able to settle out of the current, carrying interstitial fluid with them. Defining W_p to be the particle settling speed, the condition that the particles rain out of the current is given by $W_p \gtrsim |dh/dt|$. The position X of the front from the gate when this condition is first met is thus estimated to be

$$X = \sqrt{\frac{U_0 A_\ell}{W_p}} - L_0, \tag{4}$$

in which $L_0 = L_\ell / \cos\theta$ is the maximum horizontal extent of the lock.

The comparison between the measured stopping distance from the gate $X^\star$ and the prediction (4) is plotted in Fig. 5. In computing X, the value of W_p was taken to be that of the Stokes settling velocity,

$$W_p = g_p' \bar{d}_p^2 / 18\nu, \tag{5}$$

in which ν is the kinematic viscosity of water and $g_p' = g(\rho_p - \rho_0)/\rho_0$ is the reduced gravity of particles in fresh water. The 5- and 11-μm-diam ballotini are thus estimated to have a Stokes settling speed in fresh water of 0.002 and 0.009 cm/s, respectively, silicon carbide has a settling speed of 0.007 cm/s, the two smaller clays have settling speeds of 0.02 cm/s, and the largest silty clay has a settling speed of 0.07 cm/s.

The data collapse reasonably well for experiments performed using particles of the same size; the observed stopping distance relative to that predicted is found to be larger if the particle size is larger. Although (4) implicitly accounts for particle size through W_p, apparently particle size has an additional influence upon the stopping position.

There are several documented phenomena demonstrating that particle settling can be enhanced or inhibited when falling from an ambient fluid of one density into a denser lower layer. Experiments and theory examining an individual particle settling through a density interface show that its descent

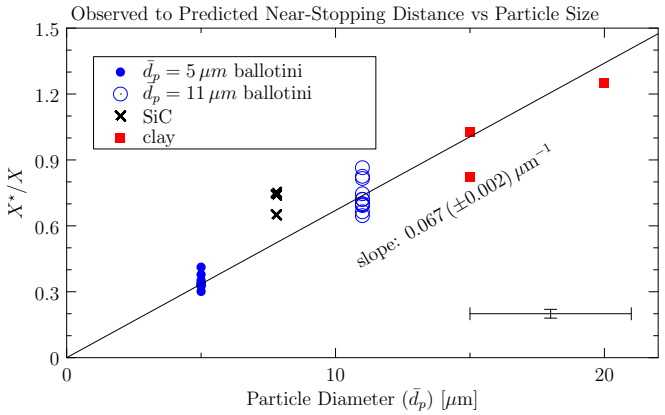

FIG. 5. Measured initial stopping distance of hypopycnal current compared with theory. The diagonal black line is the best-fit line through the data that passes through the origin. Its slope is indicated. Typical error bars for the data are indicated in the lower-right corner of the plot.

is retarded because water in the viscous boundary layer surrounding the particle is carried down with it, so reducing its buoyancy in the denser lower-layer ambient fluid [18]. Furthermore, experiments examining the settling of many particles in fresh water overlying a salty lower layer have shown collective behavior in which settling is enhanced by double diffusive convection, settling-driven convection, or, in the case of clay, flocculation [8,9,13,14,16,22,23,27].

Modeling the complex dynamics of collective particle settling is beyond the scope of this work. Rather we construct a semiempirical theory for the stopping distance using our experimental data. From the best-fit line through the points in the plot of Fig. 5, we estimate the stopping distance from the gate to be

$$X_s = (d_p/\mathcal{D}_p)X, \tag{6}$$

with $\mathcal{D}_p \simeq 15$ μm. In cases for which $X_s \gg L_0$, the correction can be interpreted as a correction to the value of W_p by a factor $(d_p/\mathcal{D}_p)^{-2}$. That is, whether the particles are small or large (but still in the Stokes regime), they collectively settle as would a single particle of diameter $\mathcal{D}_p$. This demonstrates that collective settling is playing a dominant role for particles with $\bar{d}_p \lesssim \mathcal{D}_p$. Even though the particle descent into the lower layer is inhibited because it draws down fresh water with it [18], the accumulation of many particles into descending plumes results in a larger net descent rate.

We note that the prediction (4) differs from that of Maxworthy [7] [see Eq. (15b) in that paper], who assumed that the current stopped primarily due to a balance due to the momentum flux of the current with the momentum loss due to settling particles. In that theory the net particle settling velocity was, based on measurements, assumed to be two orders of magnitude larger than the settling velocity of an individual particle and the transport of interstitial fluid by the settling particles was neglected. The resulting empirical prediction depended upon the gravity current speed, the measured settling rate, the reduced gravity of the current with respect to the ambient fluid, and a calibration depending upon the ambient fluid density relative to the interstitial (fresh water) fluid density. Both our theory and that of Maxworthy [7] necessarily have empirical parameters that account for the poorly understood dynamics of particle settling. It is our assertion that the model presented here provides a better framework for understanding these dynamics in that it indirectly accounts for the transport of interstitial fluid by settling particles and that there is only a single empirical parameter $\mathcal{D}_p$.

Next we turn to the properties of the hyperpycnal current that develops on the bottom of the tank. We expect the height of the current to be set by the depth of the ambient fluid below the stopping position of the surface current. Figure 6 compares the measured current height $H_b^\star$ with the ambient

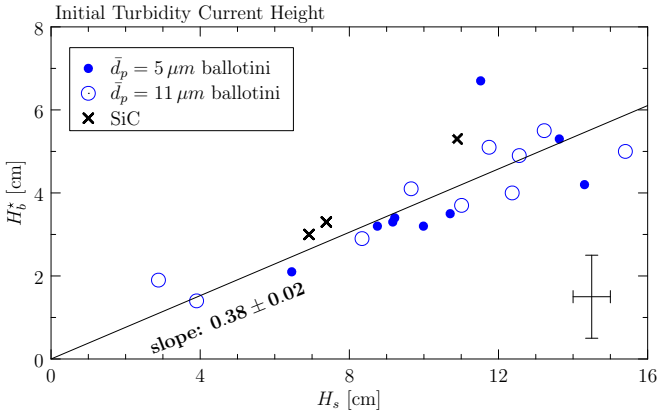

FIG. 6. Measured height of hyperpycnal current plotted against the depth of the ambient fluid at the predicted hypopycnal current stopping position from the gate. Typical error bars are indicated toward the lower right of the plot. The slope of the best-fit line through all the points is indicated.

depth at the stopping position $H_s = (L_0 + X_s)\tan\theta$, in which X_s is given by (6). Despite errors in the estimation of the slope-current height and stopping position X_s, the points lie approximately along a line of slope 0.38 ± 0.02. Thus we formulate a semiempirical relation for the height of the hyperpycnal current to be

$$H_b = (0.38 \pm 0.02)H_s. \tag{7}$$

The ratio of the hyperpycnal current depth to ambient fluid depth is moderately smaller than the value of $1/2$ predicted for steady energy-conserving gravity currents in rectangular domains [25]. This suggests that at leading order the height of the hyperpycnal current is primarily set by the competing effects of buoyancy driving the current forward and the return flow in the lee of the current setting up an adverse pressure gradient.

The speed of the hyperpycnal current that develops on the sloping bottom of the tank is assumed to be given by the current height H_b and its characteristic density relative to the ambient. We neglect the influence of buoyancy due to the fresh water being carried down by the particles within the hyperpycnal current. Thus the characteristic density of the hyperpycnal current is set primarily by the volume concentration of particles in the hyperpycnal current ϕ_b. As bourne out by comparison with observations, we take ϕ_b to be equal to the volume concentration of particles in the hypopycnal current, the assumption being that they settle uniformly and so do not change their concentration as they become manifest in the hyperpycnal current. In reality, the concentration of particles in the current must vary over its depth because of the time taken for the particles to fall a distance H_b, a depth that is much larger than the depth $h_s = A_\ell/(L_0 + X_s)$ of the hypopycnal current when it stops. With this proviso and neglecting the along-slope component of gravity acting on the current, we estimate the horizontal velocity of the hyperpycnal current to be

$$U_b = \tfrac{1}{2}\sqrt{H_b g_b'}, \tag{8}$$

in which $g_b' = g\phi_v(\rho_p - \rho_1)/\rho_1$.

The prediction for the speed of the hyperpycnal current is compared to observations in Fig. 7. Considering the crude approximations of the theory, it does remarkably well at predicting the observed speed. The speed of the hyperpycnal current is overpredicted for experiments with high concentrations of small-diameter ($\bar{d}_p = 5\ \mu$m) ballotini for which the predicted speeds are greater than 0.8 cm/s. Presumably this is because collective settling and fresh-water transport by these particles cannot be neglected in these circumstances.

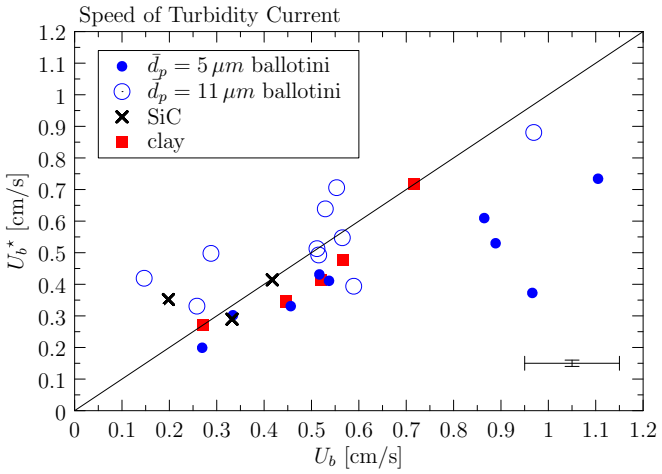

FIG. 7. Measured speed of hyperpycnal current compared with theory. Symbols represent different particle types as indicated in the legend. The diagonal line is the one-to-one line where theory matches observations. Typical error bars are shown to the bottom right of the plot.

For experiments in which the hyperpycnal current stops before reaching the end of the tank, we estimate the stopping distance to be given by the distance traveled by the current moving at speed U_b before particles fall across its depth. The total horizontal distance from the gate is thus estimated to be

$$X_b \sim X_s + \frac{U_b}{W_p} H_b, \tag{9}$$

in which W_p is the Stokes settling velocity given by (5).

The observed stopping distance is compared with theory in Fig. 8. Given the coarse assumptions throughout and leading to the final prediction (9), it is not surprising that the agreement is not particularly good. The stopping distance is consistently overpredicted, being particularly poor in the

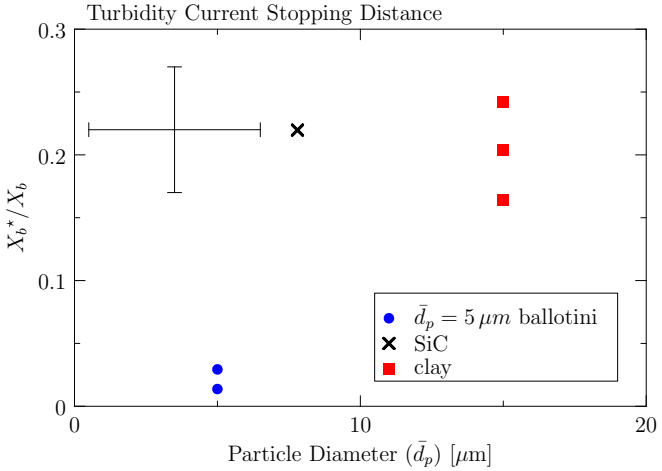

FIG. 8. Measured stopping distance of hyperpycnal current compared to predicted stopping distance. The different particle types are as indicated in the legend in Fig. 4.

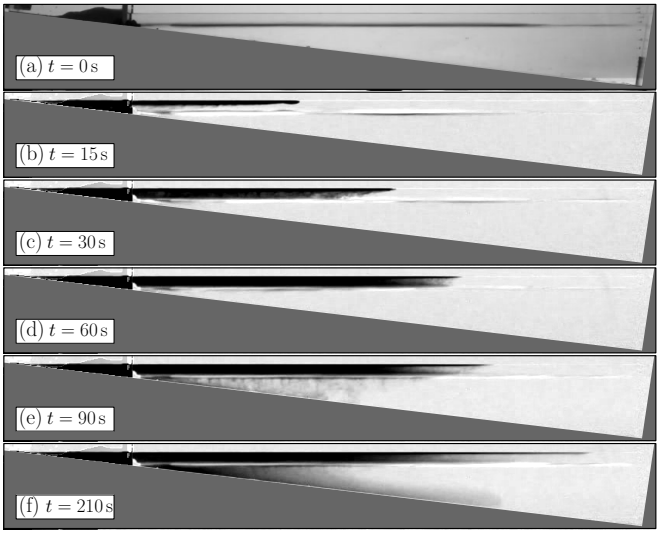

FIG. 9. Snapshots from an experiment of a hypopycnal current of fresh water with suspended glass ballotini advancing into a two-layer ambient fluid at (a) $t = 0$ s, (b) $t = 15$ s, (c) $t = 30$ s, (d) $t = 60$ s, (e) $t = 90$ s, and (f) $t = 210$ s. The experiment parameters for the tank slope, lock height, upper-layer depth, and ambient upper- and lower-layer densities, respectively, are $\theta = 8^\circ$, $H_\ell = 3.0$ cm, $H_1 = 3$ cm, $\rho_1 = 1.0300$ g/cm^3, and $\rho_2 = 1.0600$ g/cm^3. The lock fluid has 4.74 g of $\bar{d}_p = 5$ μm ballotini added to the fresh water in the lock, giving it a lock density of $\rho_\ell = 1.0094$ g/cm^3. The top image shows the unprocessed snapshot in which the interface is visualized by the dark dyeline situated at 3 cm below the surface. The snapshots below have the background intensity subtracted out in order to enhance visualization of particle settling.

case of small ballotini with $\bar{d}_p = 5$ μm. Presumably the hyperpycnal current stops sooner because the settling speed of particles is larger than the Stokes settling velocity W_p. This suggests that the collective settling behavior observed for particles leaving the hypopycnal current continues as they descend through the hyperpycnal current and that this effect is more pronounced for smaller particles.

IV. QUALITATIVE RESULTS FOR CURRENTS IN TWO-LAYER FLUID

While it is well established that a particle settling through an interface between fresh and salt water carries an envelope of fresh water with it [18], experiments of hypopycnal currents in uniform-density ambient fluid show more complicated dynamics associated with collective settling [8,9] and, in the case of clay, flocculation. In this section we show that the dynamics are further complicated when considering hypopycnal and mesopycnal currents in a stratified ambient fluid. It is our intention to demonstrate how the transport of fresh water as it is influenced by settling particles significantly changes the evolution of the current released from the lock. As for hypopycnal currents in a uniform density ambient, the microscopic dynamics are too poorly understood for us to attempt to construct a predictive model at this stage.

Two distinct experiments of particle-bearing currents in two-layer stratification are presented here. In one a hypopycnal current initially flows along the surface above an interface; in the other a mesopycnal current initially flows along the interface itself.

Figure 9 shows snapshots from the hypopycnal current experiment. The lock fluid was composed of fresh water and $\bar{d}_p = 5$ μm ballotini such that the mixture had a total density of $\rho_\ell = 1.0094$ g/cm^3. This being lighter than the upper-layer ambient fluid with density $\rho_1 = 1.0300$ g/cm^3, the current propagated along the surface and, like the case of hypopycnal currents in a uniform density ambient fluid, advanced initially at a near-constant speed of $U_s^\star = 1.99 \pm 0.07$ cm/s while its depth thinned

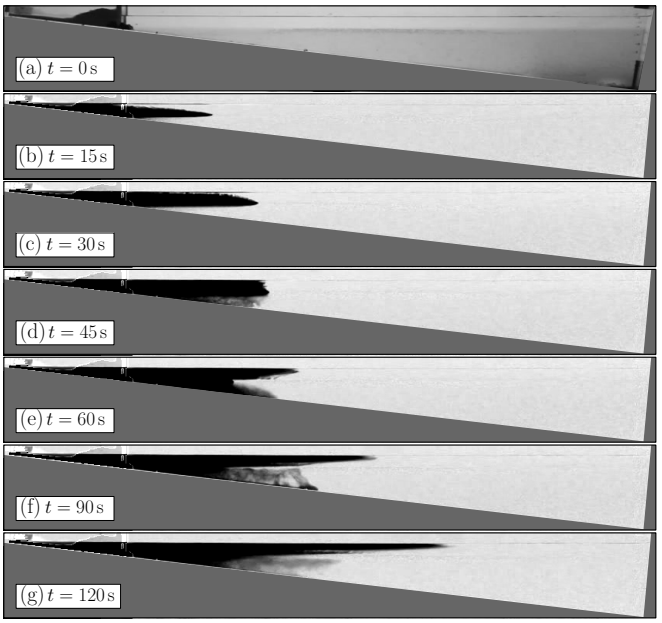

FIG. 10. Same as in Fig. 9 but showing snapshots from an experiment of a mesopycnal current of fresh water with suspended glass ballotini advancing into a two-layer ambient fluid at (a) $t = 0$ s, (b) $t = 15$ s, (c) $t = 30$ s, (d) $t = 45$ s, (e) $t = 60$ s, (f) $t = 90$ s, and (g) $t = 120$ s. The experiment parameters are $\theta = 8^\circ$, $H_\ell = 3.0$ cm, $H_1 = 3$ cm, $\rho_1 = 1.0300$ g/cm^3, and $\rho_2 = 1.0600$ g/cm^3. The lock fluid has 18.96 g of $\bar{d}_p = 5$ μm ballotini added to the fresh water in the lock, giving it a lock density of $\rho_\ell = 1.0418$ g/cm^3.

uniformly along its length [Fig. 9(b)]. Small ripples associated with internal waves at the interface were evident; however, these did not appear to affect the propagation of the current as in idealized studies of gravity currents in two-layer fluids [28–31]. Particles are observed to begin settling from the current shortly before 30 s after release [Fig. 9(c)], at which time it slowed to a near stop at a distance $X_s^\star \simeq 63$ cm from the gate.

In this two-layer experiment, the descent of the particles was temporarily arrested when they reached the interface between the upper- and lower-layer ambient fluids. Because the particle density was much larger than that of either the upper or lower layer, the near halting of their descent must have been a consequence of the particles carrying fresh water from the surface current down with them such that their net density was lighter than that of the lower layer [Fig. 9(d)]. The front of the hypopycnal current and of the interfacial current that developed below advanced slowly in the horizontal for approximately 50 s until the particles apparently shed enough of their sheath of fresh water and upper-layer ambient fluid so that their net density was greater than that of the lower layer [Fig. 9(d)]. After 90 s [Fig. 9(e)] the particles descended into the lower layer. At still later time, a hyperpycnal current developed and propagated downslope after 210 s [Fig. 9(f)], doing so with a speed $U_b^\star = 0.24 \pm 0.02$ cm/s.

The case of the mesopycnal current shown in Fig. 10 is dramatically different. Here the ambient conditions were the same as the experiment shown in Fig. 9 except that ballotini of a larger mass of $\bar{d}_p = 5$ μm were added to the lock, giving a net lock density of $\rho_\ell = 1.0418$ g/cm^3. Thus the particle mixture was more dense than the upper layer but lighter than the lower-layer ambient fluid. As expected, upon release the fluid advanced along the interface, initially having a near-constant speed of 0.58 ± 0.06 cm/s [Fig. 10(b)].

Unlike a hypopycnal current, as particles rained out of the intrusion, the upper flank of the mesopycnal current became less dense and so rose back to the surface, carrying some particles with

it [Fig. 10(c)]. This extraction of interstitial fluid and particles from the current rapidly slowed its advance. Particles descended from the bottom of the current shortly thereafter [Fig. 10(d)]. The combination of rising fluid from the upper flank of the mesopycnal current and descending particles, which also carried interstitial fluid away from its lower flank, halted the current's advance. Remarkably, the mesopycnal current front then reversed direction. This occurred because the rising fluid formed a hypopycnal current and the descending fluid formed a hyperpycnal current, both evident after 60 s [Fig. 10(e)]. The forward advance of both currents necessitated the development of a return flow between them having sufficient momentum to push the mesopycnal current backward. The hyperpycnal current itself eventually stopped as particles rained out. Interstitial fluid with some particles then rose back toward the interface around 90 s [Fig. 10(f)]. The consequent dynamics continued to be complicated with particle settling competing with rising interstitial fluid in both the upper and lower laysers [Fig. 10(g)].

V. CONCLUSION

In modern delta settings sedimentary processes tend to be ascribed either to hyperpycnal currents or to hypopycnal currents, manifest as river plumes, but how these processes may act in union has not previously been considered. The data from the lock-release experiments presented here demonstrate a greater complexity to the dynamics of settling typically supposed by sedimentary geologists. Owing to the complicated dynamics of particle settling in stratified flows, we have necessarily formulated semiempirical models for the stopping distance of the hypopycnal current as it depends upon particle diameter. This in turn was used with some success to predict the height and propagation speed of the hyperpycnal current that develops below the hypopycnal current as a result of settling particles accumulating near the bottom. While these models do not explicitly represent the dynamics of interstitial fluid being carried downward by the particles through viscous boundary layers surrounding the particles, it is clear that such dynamics have a significant influence upon the large-scale flows. In particular, a mesopycnal current is found to reverse its advance as a consequence of the rise of interstitial fluid from its upper flank and the descent of particles from its lower flank, both of which then generate return flows about the interface in order to compensate for their consequential horizontal advance along the surface and bottom of the fluid.

This idealized study is far from being a predictive model for sediment transport by river plumes which, besides being better represented by a constant-flux source, are additionally influenced by coastal currents, wind forcing, wave-induced turbulence, and Coriolis forces [1]. However, it clearly demonstrates the influence upon such large-scale flows of microscopic processes associated with particle settling. In order to improve predictions of sedimentation in delta estuaries and at the ocean floor by silts and clays originating from river plumes, particle settling should not be interpreted as a passive process.

ACKNOWLEDGMENT

This research was performed in part through funding from the Natural Sciences and Engineering Research Council of Canada.

[1] A. R. Horner-Devine, R. D. Hetland, and D. G. MacDonald, Mixing and transport in coastal river plumes, Annu. Rev. Fluid Mech. **47**, 569 (2015).

[2] T. Mulder and J. P. M. Syvitski, Turbidity currents generated at river mouths during exceptional discharges to the world oceans, J. Geol. **103**, 285 (1995).

[3] M. I. Bursik, Theory of the sedimentation of suspended particles from fluvial plumes, Sedimentology **42**, 831 (1995).

[4] J. A. Warrick, J. Xu, A. N. Marlene, and J. L. Homa, Rapid formation of hyperpycnal sediment gravity currents offshore of a semi-arid California river, Cont. Shelf Res. **28**, 991 (2008).
[5] D. J. Nowacki, A. R. Horner-Devine, J. D. Nash, and D. A. Jay, Rapid sediment removal from the Columbia river plume near field, Cont. Shelf Res. **35**, 16 (2012).
[6] J. L. Hizzett, J. E. H. Clarke, E. J. Sumner, M. J. B. Cartigny, P. J. Talling, and M. A. Clare, Which triggers produce the most erosive, frequent, and longest runout turbidity currents on deltas? Geophys. Res. Lett. **45**, 1 (2018).
[7] T. Maxworthy, The dynamics of sedimenting surface gravity currents, J. Fluid Mech. **392**, 27 (1999).
[8] J. D. Parsons, J. W. M. Bush, and J. P. M. Syvitski, Hyperpycnal plume formation from riverine outflows with small sediment concentrations, Sedimentology **48**, 465 (2001).
[9] K. Snow and B. R. Sutherland, Particle-laden flow down a slope in uniform stratification, J. Fluid Mech. **755**, 251 (2014).
[10] R. T. Bonnecaze, H. E. Huppert, and J. R. Lister, Particle-driven gravity currents, J. Fluid Mech. **250**, 339 (1993).
[11] R. T. Bonnecaze, M. A. Hallworth, H. E. Huppert, and J. R. Lister, Axisymmetric particle-driven gravity currents, J. Fluid Mech. **294**, 93 (1995).
[12] R. S. J. Sparks, R. T. Bonnecaze, H. E. Huppert, J. R. Lister, M. A. Hallworth, H. Mader, and J. Phillips, Sediment-laden gravity currents with reversing buoyancy, Earth Planet. Sci. Lett. **114**, 243 (1993).
[13] D. C. J. D. Hoyal, M. I. Bursik, and J. F. Atkinson, The influence of diffusive convection on sedimentation from buoyant plumes, Mar. Geol. **159**, 205 (1999).
[14] D. C. J. D. Hoyal, M. I. Bursik, and J. F. Atkinson, Settling-driven convection: A mechanism of sedimentation from stratified fluids, J. Geophys. Res. **104**, 7953 (1999).
[15] P. Burns and E. Meiburg, Sediment-laden fresh water above salt water: Nonlinear simulations, J. Fluid Mech. **762**, 156 (2015).
[16] S. D. Jazi and M. G. Wells, Enhanced sedimentation beneath particle-laden flows in lakes and the ocean due to double-diffusive convection, Geophys. Res. Lett. **43**, 10,883 (2016).
[17] K. Y. Yick, C. R. Torres, T. Peacock, and R. Stocker, Enhanced drag of a sphere settling in a stratified fluid at small Reynolds numbers, J. Fluid Mech. **632**, 49 (2009).
[18] R. Camassa, C. Falcon, J. Lin, R. M. McLaughlan, and N. Mykins, A first-principle predictive theory for a sphere falling through sharply stratified fluid at low Reynolds number, J. Fluid Mech. **664**, 436 (2010).
[19] A. Doostmohammadi and A. M. Ardekani, Interaction between a pair of particles settling in a stratified fluid, Phys. Rev. E **88**, 023029 (2013).
[20] A. M. Ardekani, A. Doostmohammadi, and N. Desai, Transport of particles, drops, and small organisms in density stratified fluids, Phys. Rev. Fluids **2**, 100503 (2017).
[21] M. C. Couch and E. J. Hinch, in *Physics of Granular Media*, edited by D. Bideau and J. A. Dodds (Nova Science, Hauppauge, 1991), pp. 299–321.
[22] B. R. Sutherland, K. J. Barrett, and M. K. Gingras, Clay settling in fresh and salt water, Env. Fluid Mech. **15**, 147 (2015).
[23] M. Rouhnia and K. Strom, Sedimentation from flocculated suspensions in the presence of settling-driven gravitational interface instabilities, J. Geophys. Res. **120**, 6384 (2015).
[24] A. J. Hogg, H. E. Huppert, and M. A. Hallworth, Reversing buoyancy of particle-driven gravity currents, Phys. Fluids **11**, 2891 (1999).
[25] T. B. Benjamin, Gravity currents and related phenomena, J. Fluid Mech. **31**, 209 (1968).
[26] J. O. Shin, S. B. Dalziel, and P. F. Linden, Gravity currents produced by lock exchange, J. Fluid Mech. **521**, 1 (2004).
[27] F. Blanchette and J. W. M. Bush, Particle concentration evolution and sedimentation-induced instabilities in a stably stratified environment, Phys. Fluids **17**, 073302 (2005).
[28] J. Y. Holyer and H. E. Huppert, Gravity currents entering a two-layer fluid, J. Fluid. Mech. **100**, 739 (1980).

[29] B. R. Sutherland, P. J. Kyba, and M. R. Flynn, Interfacial gravity currents in two-layer fluids, J. Fluid Mech. **514**, 327 (2004).
[30] M. R. Flynn and P. F. Linden, Intrusive gravity currents, J. Fluid Mech. **568**, 193 (2006).
[31] M. R. Flynn, M. Ungarish, and A. W. Tan, Gravity currents in a two-layer stratified ambient: The theory for the steady-state (front condition) and lock-released flows, and experimental confirmations, Phys. Fluids **24**, 026601 (2012).